

# Elliptic flow fluctuations in Au+Au collisions at $\sqrt{s_{NN}} = 200$ GeV

P. Sorensen<sup>a</sup> for the STAR Collaboration\*

<sup>a</sup>Brookhaven National Laboratory, Upton, New York 11973-5000, USA

In this talk, we report an analysis of elliptic flow ( $v_2$ ), non-flow ( $\delta_2$ ), and  $v_2$  fluctuations ( $\sigma_{v_2}$ ) for the STAR collaboration at middle rapidity in  $\sqrt{s_{NN}} = 200$  GeV Au+Au collisions. We compare the results to models of the fluctuations in the initial eccentricity of the overlap zone.

*Introduction:* Understanding the early-time dynamics in heavy-ion collisions is an important step in understanding the properties of the matter created in the collision overlap zone. Elliptic flow ( $v_2$ ) measurements are sensitive to the shape of the initial overlap zone [1] so  $v_2$  fluctuations can reveal information about fluctuations and correlations in the initial geometry. Those fluctuations and correlations will lead to a better understanding of the initial conditions of the collision evolution. We report on a study of  $v_2$  fluctuations based on 15 million events measured with the STAR detector [2]. A similar analysis has been carried out by PHOBOS [3] and results have been discussed in the literature [4]. Please note, data shown in this talk, showing small  $v_2$  for events containing jets, was in error.

*Analysis method:* The q-distribution method can be used to gain access to information about azimuthal correlations and  $v_2$  fluctuations. The  $n^{th}$  harmonic reduced flow vector is defined as  $q_{n,x} = \frac{1}{\sqrt{M}} \sum_i \cos(n\phi_i)$  and  $q_{n,y} = \frac{1}{\sqrt{M}} \sum_i \sin(n\phi_i)$ , where  $M$  is the number of tracks and  $\phi_i$  is the azimuth angle of a track with respect to a preferred emission axis [5]. The sums over the x and y components of the particle momentum are equivalent to random walks so that the central limit theorem is applicable for large  $M$ , in which case the  $\vec{q}_n$  distribution will be a 2-D Gaussian with widths that depend on particle correlations and  $v_2$  fluctuations. According to the definition of  $v_2$ , if the reaction-plane is the preferred axis, the 2-D Gaussian will be shifted along  $x$  by  $\sqrt{M}v_n$  with widths:  $\sigma_x^2 \simeq \frac{1}{2}(1 + M\delta_n)$  and  $\sigma_y^2 \simeq \frac{1}{2}(1 - M\delta_n)$ .  $\delta_n = \langle \cos(n\Delta\phi) \rangle - v_n^2$  are correlations unrelated to the reaction plane [5]. Neither the preferred axis, nor the reaction plane direction are known on an event-by-event basis, so we calculate the magnitude  $|q_n|$ . The 2-D Gaussian then becomes:

$$\frac{dN}{q_n dq_n} = \frac{\exp\left(-\frac{q_n^2 + Mv_n^2\{q\}}{2\sigma_x^2}\right)}{\sqrt{\pi}\sigma_x\sigma_y} \sum_{k=0,2,\dots}^{\infty} \left(1 - \frac{\sigma_x^2}{\sigma_y^2}\right)^k \left(\frac{q_n}{v_n\{q\}\sqrt{M}}\right)^k \frac{1}{k!} \Gamma\left(\frac{2k+1}{2}\right) I_k\left(\frac{q_n v_n\{q\}\sqrt{M}}{\sigma_x^2}\right) \quad (1)$$

where  $\Gamma$  and  $I_k$  are gamma and modified Bessel's functions. If we assume the preferred axis for the  $dN/d|q|$  is the reaction-plane, then  $v_2\{q\} = v_2$  and  $v_2$  fluctuations can be introduced by convoluting the above distribution with a  $v_2$  distribution ( $dN/dv_2$ ). This

\*For the full list of STAR authors and acknowledgements, see appendix 'Collaborations' of this volume

introduces an added width to  $dn/d|q_2|$ :  $\sigma_x^2 \simeq \frac{1}{2} (1 + M\delta_2 + 2M\sigma_{v_2}^2)$ , where  $\sigma_{v_2}$  is the r.m.s. width of  $dN/dv_2$ .  $\delta_2$  and  $\sigma_{v_2}^2$  contribute to the width with a factor of  $M$ , so it is not possible to extract these quantities independently as previously thought [6]. Rather, we define the dynamic width of  $dN/d|q_2|$  as  $\sigma_{dyn}^2 = \delta_2 + 2\sigma_{v_2}^2$ , which can be readily extracted from data.

We don't know a priori what the preferred emission axis is. For peripheral Au+Au or p+p collisions, the preferred axis may be predominantly determined by the thrust axis of outgoing partons. However, for mid-central and central collisions, the four-particle cumulant  $v_2\{4\}$  (a higher multiplicity correlation analysis [7]) decreases with eccentricity suggesting the geometry of the overlap determines the preferred axis.

Distinguishing between  $\sigma_{v_2}^2$  and  $\delta_2$  requires knowledge of the reaction-plane or information about the  $\Delta\phi$ -,  $\Delta\eta$ -, charge-sign- or multiplicity-dependence of non-flow. STAR addresses this in two general ways, 1) analyzing higher multiplicity correlations as in a q-distribution or higher order cumulant analysis [7, 1] or 2) analyzing the  $\Delta\phi$ ,  $\Delta\eta$ , or charge-sign dependence of correlations. Examples of 2) include measuring two-particle correlations across a wide  $\eta$ -gap [8], correlating only like-sign particles, or by fitting the  $\Delta\phi$ ,  $\Delta\eta$  correlation density to isolate the  $\cos 2(\Delta\phi)$  term  $v_2\{2D\}$  [9]. But the small  $\Delta\phi$  correlations in Au+Au collisions stretch over a large  $\Delta\eta$  range [10] and it's possible that the space-momentum correlation inducing mechanism responsible for  $v_2$  may contribute to the near-side correlation by translating quantum- or geometry-fluctuations from the initial overlap to correlations in momentum-space [11, 12] linking the ridge and  $v_2$  [13].

For  $dN/dv_2$ , we consider a Gaussian and Bessel-Gaussian (BG( $v_{BG}$ ,  $\sigma_{v_{BG}}$ )) [16]. Convolved with Eq. 1, both give an equally good description of  $dN/d|q|$ . The mean and r.m.s. of the BG or the parameters  $v_{BG}$  and  $\sigma_{v_{BG}}$  can be reported. We find that the BG mean and r.m.s. are within errors the same as the Gaussian mean and r.m.s. The use of a BG shape for the  $dN/dv_2$  is motivated by the shape of the participant eccentricity [15] distribution in a Glauber Monte Carlo model [14]. In the case that  $v_2 \propto \varepsilon_2$ , the parameters extracted from the BG are either related to the participant-plane or the reaction-plane. The parameter  $v_{BG}$  represents the  $v_2$  computed with respect to the reaction-plane, while  $\langle v_2 \rangle$  represents  $v_2$  computed with respect to the participant-plane [16]. Here, we report the mean and rms width of a Gaussian and compare it to models of  $\varepsilon_{part}$ .

*Results:* Fig. 1 (left) shows our fits to  $dN/d|q_2|$  where  $|q_2|$  is calculated from three track samples: full-acceptance ( $q\{\text{full}\}$ ), reduced-acceptance ( $q\{\eta/2\}$ ), and full-acceptance like-sign ( $q\{\text{like-sign}\}$ ). The different samples are expected to contain different contributions of correlations; HBT, resonance decays, and parton fragments, which contribute to non-zero values of  $\delta_2$ . The inset shows the ratio of each distribution to  $dN/d|q\{\text{full}\}|$ . The widths are ordered as follows:  $\sigma_{dyn}\{q\{\eta/2\}\} > \sigma_{dyn}\{q\{\text{full}\}\} > \sigma_{dyn}\{q\{\text{like-sign}\}\}$ . This is expected because the like-sign sample removes most correlations caused by resonance decay. Jet fragments exhibit charge-ordering so those correlations are also reduced. The  $\eta/2$  sample gives a greater weight to the short-range correlations so  $\delta_2$  is enhanced.

Fig. 1 (right) shows the dynamic width of the full-acceptance  $dN/d|q|$ . The tan band includes systematic uncertainties from acceptance, finite multiplicity and comparisons of methods including the dynamic width from the cumulants  $v_2\{2\}^2 - v_2\{4\}^2 = \delta_2 + 2\sigma_{v_2}^2$ . It was shown in ref. [16] that within the precision of our measurements we cannot extract more information from  $dN/d|q|$  than that already found from the cumulants. In particular,

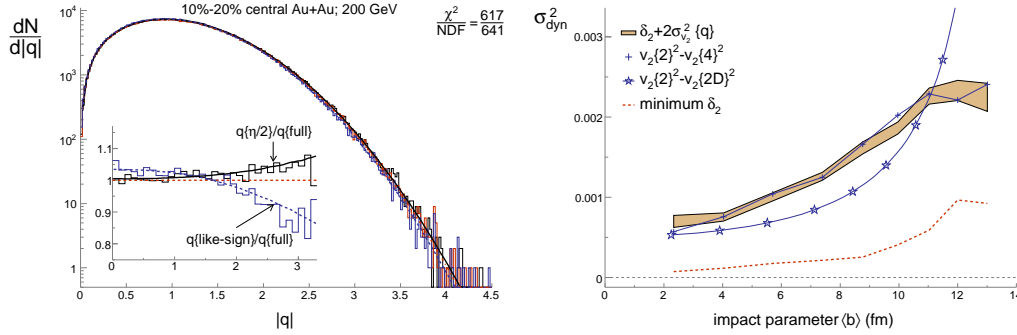


Figure 1. Left:  $dN/d|q|$  for like-sign tracks ( $q\{\text{like-sign}\}$ ), tracks within one hemisphere of the STAR acceptance ( $q\{\eta/2\}$ ), and all tracks with  $0.15 < p_T < 2.0$  GeV/c ( $q\{\text{full}\}$ ). The inset shows the ratio of each distribution to  $q\{\text{full}\}$ . Right: The dynamic width of  $dN/d|q|$  with width from cumulant analysis.  $v_2\{2\}^2 - v_2\{2D\}^2$  gives the non-flow  $\delta_2$  inferred from a fit to the 2D correlation densities [9].

if the  $v_2$  fluctuations are Gaussian, then the equality  $v_2\{2\}^2 - v_2\{4\}^2 = \delta_2 + 2\sigma_{v_2}^2$  is exact. Published STAR  $v_2\{2\}$  and  $v_2\{4\}$  values vs. centrality have been calculated by weighting each event by the number of tracks in the event [1]. Those are not comparable to the  $q$ -distribution analysis where each event is weighted equally. We therefore compare to cumulant data without the multiplicity weighting and find good agreement. The minimum value of  $\delta_2$  shown in Fig. 1 (right) is calculated from the difference between  $\langle q*q \rangle$  calculated with same-charge pairs and unlike-sign pairs. We also show  $\delta_2\{2D\} = v_2\{2\}^2 - v_2\{2D\}^2$  which shows that a large component of  $\sigma_{dyn}^2$  is accounted for by the near-side peak in the 2D correlations [9]. Fig. 2 (left) shows the allowed values for  $\langle v_2 \rangle$  and  $\sigma_{v_2}$ . The case of zero fluctuations is not excluded and an upper limit is reported.

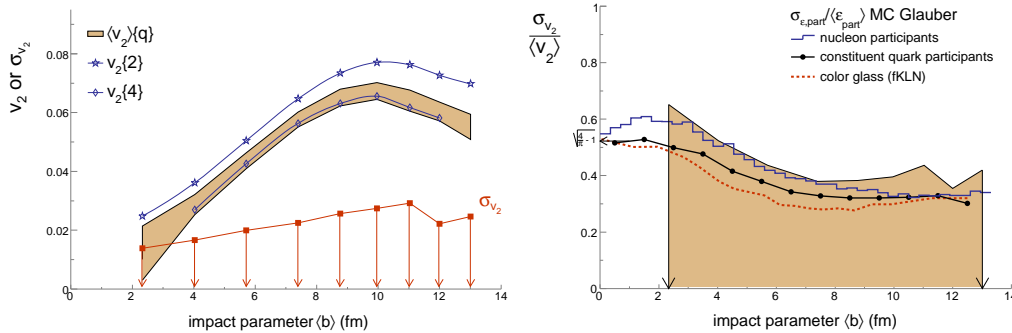


Figure 2. Left: The tan band shows the allowed values of  $\langle v_2 \rangle$  from this analysis and the upper limit on  $\sigma_{v_2}$ . Right: Upper limit on  $\sigma_{v_2}/\langle v_2 \rangle$  compared to models of eccentricity.

Fig. 2 (right) shows  $\sigma_{v_2}/\langle v_2 \rangle$  calculated using a Gaussian for  $dN/dv_2$ . The upper limit on this ratio is compared to several Monte Carlo models of  $\varepsilon_{part}$  fluctuations. In the nucleon Glauber models, the eccentricity  $\varepsilon = \langle y^2 - x^2 \rangle / \langle y^2 + x^2 \rangle$  is calculated based on the  $x$  and  $y$  coordinates of participant nucleons. For the constituent quark Glauber model,

each nucleon is treated as three constituent quarks bound within the nucleon, and the eccentricity is calculated based on the constituent quarks that participate in the collision. All models lie within the allowed range while the CGC model [17] and the model based on constituent quarks both have smaller relative widths. The nucleon participant model leaves little room for other sources of fluctuations and correlations beyond the initial geometric ones. The large near-side peak observed in two-particle correlations contradict the idea that all or most of the width of  $\sigma_{dyn}^2$  is dominated by  $\sigma_{v_2}$  suggesting that the CGC or constituent-quark model may be preferred. Recently it was proposed that correlations and fluctuations in the initial conditions may also contribute to the near-side ridge [12].

*Conclusions:* The dynamic width of  $dN/dq$  has been presented. The width reflects correlations and  $v_2$  fluctuations. An upper limit on  $\sigma_{v_2}$  has been presented and compared to models of  $\varepsilon_{part}$  fluctuations. From our comparison to the Glauber MC we conclude that either the density fluctuations in the initial state are manifested in both the near-side peak and in  $\sigma_{v_2}$ , or the initial overlap density is smoother than would be expected from a Glauber model.

## REFERENCES

1. K. H. Ackermann *et al.* [STAR Collaboration], Phys. Rev. Lett. **86**, 402 (2001); C. Adler *et al.* [STAR Collaboration], Phys. Rev. Lett. **89**, 132301 (2002); J. Adams *et al.* [STAR Collaboration], Phys. Rev. Lett. **92**, 052302 (2004); J. Adams *et al.* [STAR Collaboration], Phys. Rev. C **72**, 014904 (2005); J. Adams *et al.* [STAR Collaboration], Phys. Rev. Lett. **95**, 122301 (2005).
2. STAR Collaboration, C. Adler *et al.*, Nucl. Instr. Meth. A **499**, 624 (2003).
3. B. Alver *et al.* [PHOBOS Collaboration], arXiv:nucl-ex/0702029; B. Alver *et al.*, Phys. Rev. C **77**, 014906 (2008); B. Alver *et al.* [PHOBOS Collaboration], Int. J. Mod. Phys. E **16**, 3331 (2008).
4. S. Mrowczynski and E. V. Shuryak, Acta Phys. Polon. B **34**, 4241 (2003); X. I. J. Zhu, M. Bleicher and H. Stoecker, Phys. Rev. C **72**, 064911 (2005); S. Vogel, G. Torrieri and M. Bleicher, arXiv:nucl-th/0703031; W. Broniowski, P. Bozek and M. Rybczynski, Phys. Rev. C **76**, 054905 (2007); R. Andrade, F. Grassi, Y. Hama, T. Kodama and O. J. Socolowski, arXiv:nucl-th/0608067; R. Peterson G. Andrade, F. Grassi, W. L. Qian, T. Osada, C. E. Aguiar and T. Kodama, arXiv:0711.4544 [hep-ph].
5. J. Y. Ollitrault, arXiv:nucl-ex/9711003; A. M. Poskanzer and S. A. Voloshin, Phys. Rev. C **58**, 1671 (1998); N. Borghini, P. M. Dinh and J. Y. Ollitrault, Phys. Rev. C **63**, 054906 (2001).
6. P. Sorensen [STAR Collaboration], J. Phys. G **34**, S897 (2007).
7. C. Adler *et al.* [STAR Collaboration], Phys. Rev. C **66**, 034904 (2002).
8. S. A. Voloshin [STAR Collaboration], AIP Conf. Proc. **870**, 691 (2006); S. A. Voloshin [STAR Collaboration], J. Phys. G **34**, S883 (2007).
9. T. A. Trainor and D. T. Kettler, arXiv:0704.1674 [hep-ph]. M. Daugherty these proceedings.
10. J. Adams *et al.* [STAR Collaboration], J. Phys. G **32**, L37 (2006); J. Adams *et al.* [STAR Collaboration], Phys. Rev. C **73**, 064907 (2006); J. Putschke, J. Phys. G **34**, S679 (2007); J. Adams *et al.* [Star Collaboration], Phys. Rev. C **75**, 034901 (2007).

11. S. A. Voloshin, Phys. Lett. B **632**, 490 (2006); C. A. Pruneau, S. Gavin and S. A. Voloshin, Nucl. Phys. A **802**, 107 (2008).
12. A. Dumitru, F. Gelis, L. McLerran and R. Venugopalan, arXiv:0804.3858 [hep-ph].
13. R. C. Hwa and C. B. Yang, arXiv:0801.2183 [nucl-th].
14. M. Miller and R. Snellings, arXiv:nucl-ex/0312008.
15. S. Manly *et al.* [PHOBOS Collaboration], Nucl. Phys. A **774**, 523 (2006); R. S. Bhalerao and J. Y. Ollitrault, Phys. Lett. B **641**, 260 (2006).
16. S. Voloshin, A. Poskanzer, A. Tang and G. Wang, Phys. Lett. B **659**, 537 (2008).
17. H. J. Drescher and Y. Nara, Phys. Rev. C **76**, 041903 (2007).